

NON-LINEAR HARMONICS OF A SEEDED FEL AT THE WATER WINDOW AND BEYOND

G. Penco[†], E. Allaria, L. Badano, F. Bencivenga, A. Brynes, C. Callegari, F. Capotondi, A. Caretta, P. Cinquegrana, M.B. Danailov, D. De Angelis, A. Demidovich, S. Di Mitri, L. Foglia, G. Gaio, A. Gessini, L. Giannessi, G. Kurdi, M. Manfreda, M. Malvestuto, C. Masciovecchio, R. Mincigrucci, I. Nikolov, E. Pedersoli, S. Pelli Cresi, E. Principi, P. Rebernik, A. Simoncig, S. Spampinati, C. Spezzani, M. Trovò, M. Zangrando, G. De Ninno
Elettra – Sincrotrone Trieste SCpA, Basovizza, Italy
G. Perosa, F. Sottocorona, Università degli Studi di Trieste, Trieste, Italy
S. Dal Zilio, Istituto Officina dei Materiali, Consiglio Nazionale delle Ricerche, Trieste, Italy
V. Chardonnet, M. Hennes, B. Vodungbo, E. Jal, Sorbonne Université, CNRS, Laboratoire de Chimie Physique-Matière et Rayonnement, France
J. Lüning Helmholtz-Zentrum Berlin für Materialien und Energie GmbH, Berlin, Germany
P. Bougiatioti, C. David, B. Roesner, Paul Scherrer Institut, Villigen PSI, Switzerland
M. Sacchi, Institut des NanoSciences de Paris, CNRS, Sorbonne Université, Paris, France and Synchrotron SOLEIL, L'Orme des Merisiers, Saint-Aubin, Gif-sur-Yvette, France
E. Roussel, PhLAM/CERLA, Villeneuve d'Ascq

Abstract

The advent of free electron lasers (FELs) in the soft and hard X-ray spectral region has opened the possibility to probe electronic, magnetic and structural dynamics, in both diluted and condensed matter samples, with femtosecond time resolution. In particular, FELs have strongly enhanced the capabilities of several analytical techniques, which take advantage of the high degree of transverse coherence provided. FELs based on the harmonic up-conversion of an external seed laser are also characterised also by a high degree of longitudinal coherence, since electrons inherit the coherence properties of the seed. At the present state of the art, the shortest wavelength delivered to user experiments by an externally seeded FEL light source is about 4 nm. We show here that pulses with a high longitudinal degree of coherence (first and second order) covering the water window and with photon energy extending up to 790 eV can be generated by exploiting the so-called nonlinear harmonic regime, which allows generation of radiation at harmonics of the resonant FEL wavelength.

Moreover, we report the results of two proof-of-principle experiments: one measuring the oxygen K-edge absorption in water (~ 530 eV), the other analysing the spin dynamics of Fe and Co through magnetic small angle x-ray scattering at their L-edges (707 eV and 780 eV).

INTRODUCTION

The high degree of transverse coherence of the FELs pulses has been exploited by several techniques, including Fourier transform holography, coherent diffraction imaging, and ptychography. In the case of a seeded FEL, the output radiation has been proven to have also a high degree of longitudinal coherence [1-3] that is of crucial

importance for techniques such as linear and nonlinear spectroscopies and coherent control, requiring both phase and wavelength manipulation within a given pulse. In a seeded FEL operating in High Gain Harmonic Generation (HG) mode [4] an external seed laser imprints an energy modulation on an electron beam passing through an undulator (called modulator). Then, the electrons are sent through a magnetic dispersive section that converts this energy modulation into a density modulation, known as bunching, whose spectral content includes higher harmonics of the seed, with a progressively fading coefficient [5]. The electron beam is then injected into an undulator tuned to be resonant to a given harmonic of the seed: since the process is stimulated by the seed laser, all electrons emit in phase, resulting in the generation of nearly Fourier-transform-limited pulses. The reduction of the bunching with the increase of the harmonic order sets a limit on the shortest wavelength that can be generated. In fact, the bunching level at the desired harmonic has to be substantially larger than the shot noise, in order to avoid the Self Amplified Spontaneous Emission (SASE) process becoming dominant, thereby spoiling the longitudinal coherence of the FEL output.

The HG scheme has been implemented at FERMI in a two-stage cascade, using the emission from the first stage to seed the second one. In this configuration the shortest wavelength delivered to users for experiments is about 4nm [6-8], corresponding to the 65th harmonic of an ultraviolet laser. The possibility to reach a similar spectral regime in a single stage FEL by adopting the echo-enabled harmonic generation (EEHG) scheme [9] has been recently proven. Moreover, coherent and stable emission at 2.6 nm (~474 eV) was observed [10], although the parameters used for the experiment allowed only a feeble intensity, comparable to the broadband spontaneous emission coming from the whole electron bunch.

[†] giuseppe.penco@elettra.eu

In order to extend the FERMI tuning range into the water window and up to the L-edge of the 3d transition metals (up to ~ 800 eV), we exploit at FERMI the nonlinear harmonic generation (NHG) regime [11,12]. This is based on the fact that the exponential gain leading to the emission at the harmonic λ_n drives the bunching also at its harmonics $\lambda_m = \lambda_n/m$, where m is an integer, with the consequent generation of light at λ_m .

In this paper, we report the generation of the third nonlinear harmonic at about 700-800 eV and at the oxygen K-edge (~ 530 eV), as well as the characterization of this radiation component in terms of spectral purity, pulse energy and longitudinal coherence [13]. In particular, we show that the high coherence properties of the seed laser are transferred to both the fundamental FEL wavelength and its nonlinear harmonics.

FEL PULSE CHARACTERIZATION AT 530 eV AND AT 700-800 eV

The experiment described below was carried out at the FERMI FEL-2 line, which is based on two HGHG stages, operating in the fresh bunch mode [14]. In the case of circularly polarized light, all nonlinear harmonics are emitted off axis, while in linear polarization only odd harmonics are emitted on axis. We focused on the third nonlinear harmonic emission and we set the fundamental wavelength with a linear horizontal polarization. In the following, we report one of the cases of interest: the third harmonic of 5.3 nm, i.e. 1.77 nm, corresponding to the Co L-edge (~ 700 eV). Changing the seed laser wavelength from 240 to 260 nm and tuning accordingly the radiator gap, it was also possible to lase in third harmonic also at the Fe L-edge (~ 780 eV) obtaining a similar performance.

The electron beam energy was set to 1.488 GeV. The bunch charge was 600 pC and the bunch duration (FWHM) about 0.9 ps (corresponding to a peak current of about 800 A). The FEL-2 first stage was tuned to be resonant at 21.2 nm (12th harmonic of a 254.4 nm seed laser) and the second stage at 5.3 nm (4th harmonic).

To estimate the pulse energy of the output radiation at 700 eV, we used a calibrated photodiode and a set of solid-state filters to minimize contributions from undesired radiation (i.e., the seed laser and the emission from the first stage). Inserting different kinds of solid-state filters with known transmission curves it was possible to estimate a pulse energy of about 19.4 μ J at 233 eV (with a rms uncertainty of 0.1 μ J) and 150 nJ at 700 eV (with a rms uncertainty of 100 nJ). The derived estimation is in good agreement with the typical ratio of 1% documented in literature [15] and expected from simulations. More details are reported in [13].

Two spectrometers were used to characterize simultaneously the FEL emission at the fundamental (5.3 nm, 233 eV) and at the third nonlinear harmonic (1.77 nm, 700 eV) on a shot-to-shot basis: one (called PRESTO) [16] integrated in the common photon transport line of the FERMI experimental hall and one (called WEST) installed downstream of the EIS-TIMEX end station [17]. The FEL

gain curves at 233 eV and at 700 eV were measured by progressively detuning the undulator gap of the second stage radiator and taking the shot-to-shot integrated signal of the PRESTO and WEST spectrometers. The obtained results were scaled according to the pulse energy estimation mentioned above, and compared with numerical simulations run with GENESIS 1.3 [18] (see Fig. 1).

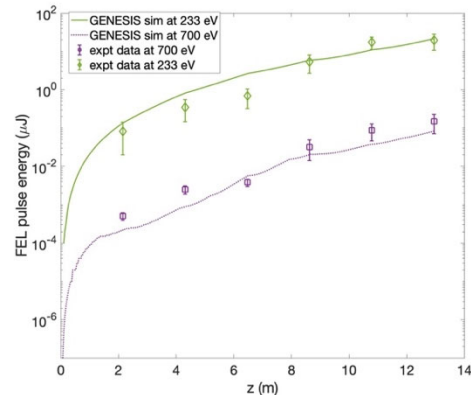


Figure 1: Measured (markers) and GENESIS simulated (lines) FEL gain curves at 233 eV and at 700 eV. Error bars correspond to the standard deviation from the mean value calculated over 50 shots.

Simulations are in good agreement with the measurements. The harmonic growth results in fact from the sum of a linear and a nonlinear contribution; the former dominates in the first part of the radiator, where as a result of the seeding there is a non-negligible bunching also at the harmonic of the resonant wavelength. When the fundamental field grows along the radiator, it contributes to the increase of the electron bunching at its harmonics, entering into a nonlinear regime and sustaining the harmonic gain. The relevant contribution to the harmonic amplification coming from the fundamental growth is confirmed by the GENESIS simulation: if the latter is artificially suppressed, the harmonic field is reduced by about 50%.

The spectral quality of the nonlinear harmonic at 700 eV was studied by acquiring 400 consecutive single-shot spectra (see Fig. 2). The statistics over the FEL bandwidth (see Fig. 2d) reveal that the largest fraction of shots have a relative FWHM bandwidth smaller than 0.1%. However, residual microbunching instabilities can be responsible for a certain broadening of the FEL spectrum and in fact numerical simulations foresee an unstructured FEL pulse with a relative FWHM bandwidth of a few 10^{-4} . Microbunching instabilities are usually damped by the laser-heater (LH) system [19] and in an optimized condition the maximum FEL intensity is obtained with a LH pulse energy of about 1 μ J. Increasing the LH power beyond this value causes the larger induced energy spread to lower the FEL gain and consequently to decrease the FEL intensity, but at the same time damping the residual microbunching instabilities. We show in [13] that with a trade-off LH pulse energy of 2.7 μ J, the average FEL bandwidth is reduced, with a significant fraction of shots

(about 20%) exhibiting a relative FWHM bandwidth of 0.05%, approaching the ideal case resulting from the simulations.

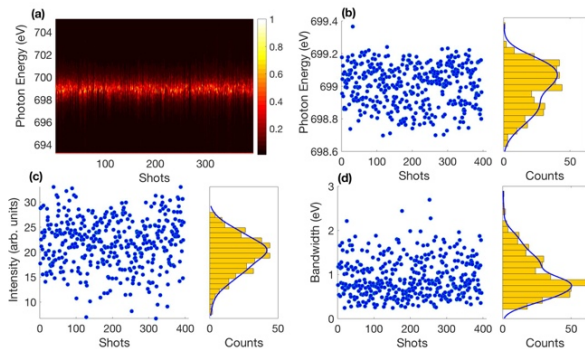


Figure 2: (a) Series of 400 consecutive single-shot spectra at 700 eV acquired with the PRESTO spectrometer. Also shown are the statistics of (b) the central wavelength stability, (c) the spectral intensity, and (d) the FWHM spectral bandwidth.

A similar spectra characterization was performed tuning the fundamental at 7 nm in linear horizontal polarization and measuring the spectra of the third nonlinear harmonic at 2.33 nm (~ 530 eV), corresponding to the oxygen K-edge [13].

LONGITUDINAL COHERENCE

The statistical properties of the light emitted by a seeded FEL differ substantially from those of a SASE FEL source: the former resembles those of laser light [20], while SASE has the typical statistics of chaotic light [21]. We used the statistics of the spectra acquired at 530 eV and at 700 eV to calculate the normalized second-order correlation function $g^{(2)}$, defined in [22], as

$$g^{(2)}(\lambda_1, \lambda_2) = \frac{\langle I(\lambda_1)I(\lambda_2) \rangle}{\langle I(\lambda_1) \rangle \langle I(\lambda_2) \rangle}, \quad (1)$$

where $I(\lambda_1)$ and $I(\lambda_2)$ are spectral intensities at different wavelengths measured simultaneously and the angular brackets indicate averaging over a large ensemble of different radiation pulses.

In the literature, it is very common to represent $g^{(2)}$ as a function of $\Delta\lambda = \lambda_1 - \lambda_2$. The value of $g^{(2)}(\Delta\lambda = 0)$, generally indicated as $g^{(2)}(0)$ is 1 for a fully coherent source. FERMI has been proven to provide laser-like output with $g^{(2)}(0)$ close to 1 [20], while SASE FELs are characterized by $g^{(2)}(0) \approx 2$ [23].

We have analysed the spectra acquired at 533 eV and 700 eV and calculated the $g^{(2)}$ function, averaged over a very narrow central bandwidth ($\Delta\lambda = 3 \times 10^{-4}$ nm) and over a larger interval ($\Delta\lambda = 1.5 \times 10^{-3}$ nm). The value found was of $g^{(2)}(0) \sim 1.16$ and was almost independent of the bandwidth chosen (Fig. 3). In both cases, narrow and broader range, it was very close to the typical performance obtained at FERMI in the nominal spectral range (see [13] for more details). This supports the theory indicating that the high coherence properties of the seed laser are transferred not only to the fundamental FEL wavelength but also to its nonlinear harmonics.

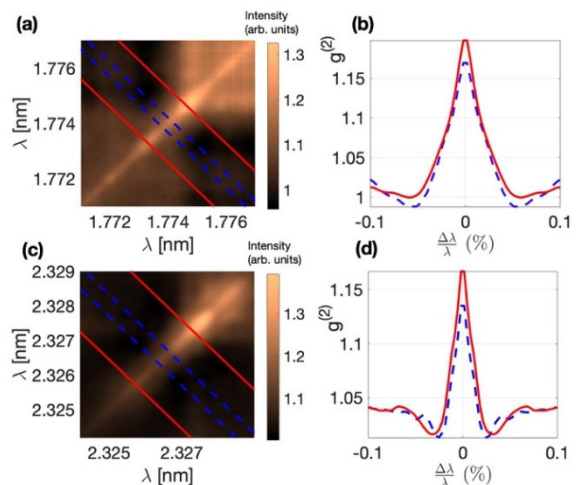


Figure 3: Measurements of the $g^{(2)}$ function for 700 eV (1.77 nm) and 530 eV (2.33 nm) radiation: (a) and (c) the $g^{(2)}$ function calculated as defined in Eq. (1) for the two different photon energies and (b) and (d) the mean values of $g^{(2)}$ calculated by averaging over a very narrow central bandwidth (blue dotted line) and over a larger one (red solid line).

PROOF OF PRINCIPLE EXPERIMENTS

To demonstrate that nonlinear harmonics generated by a seeded FEL can find useful applications, we report the results of two proof-of-principle experiments.

X-Ray Absorption Spectroscopy of Water Across the Oxygen K-edge

The x-ray-absorption spectroscopy (XAS) spectrum of steady room-temperature water across the oxygen K edge (~ 535 eV) has been measured at the EIS-TIMEX beamline in the spectral region 530–545 eV operating in transmission geometry [13].

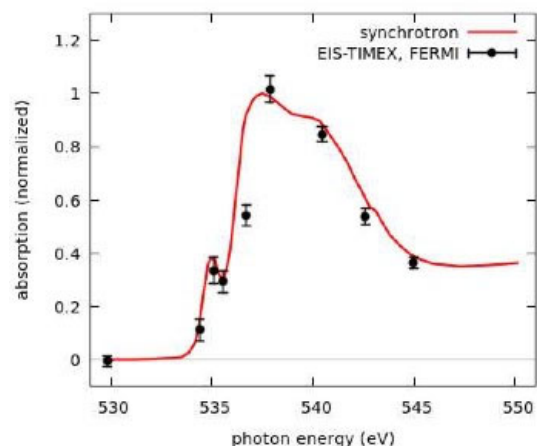


Figure 4: Normalized XAS at the O K-edge measured in transmission geometry with the nonlinear harmonics FEL generated at FERMI (black circles) compared with a similar measurement performed at the SSRL synchrotron (red continuous line).

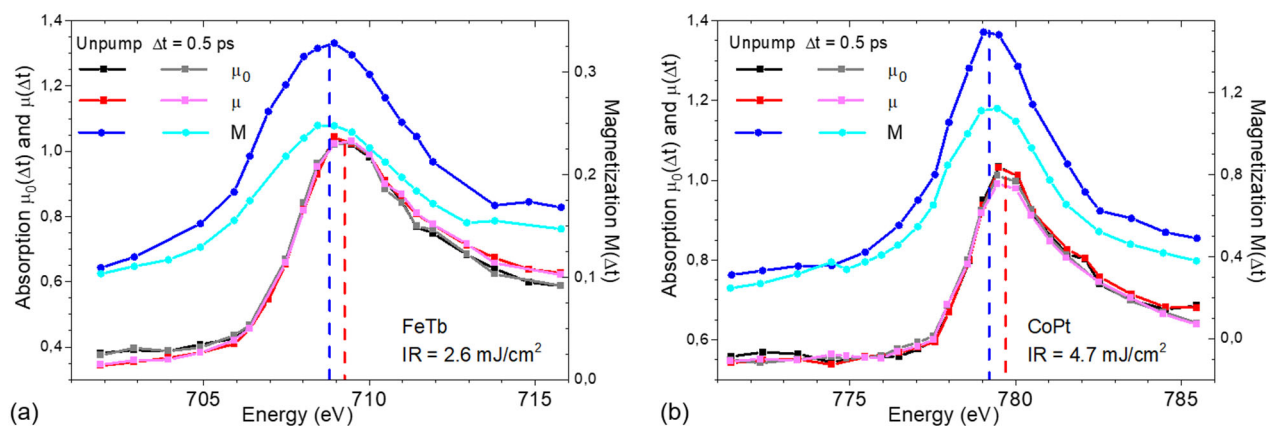


Figure 5: Absorption spectrum at Fe L_3 -edge without pumping (red) and after 0.5-ps IR-laser pulse with an average energy density of 2.6 mJ/cm^2 (magenta). Black and grey lines are reference static absorption spectra simultaneously collected in a nearby unpumped area of the sample. The blue and cyan lines show the magnetic scattering efficiency without optical pump and 0.5 ps after pumping, respectively (right scale). (b) same as (a) for CoPt sample at the Co L_3 -edge for a pump IR laser average energy density of 4.7 mJ/cm^2 . The data show that while the XAS signal is minimally affected by the optical excitation, the magnetic signal is strongly reduced after the optical stimulus.

The water sample was confined in a sealed microfluidic cell, with thin Si 3 N 4 windows (100-nm thickness) transparent to the soft x-ray radiation. For each photon energy, the spectral line was measured by integrating 1500 shots. The results are plotted in Fig. 4: the high wavelength stability of FERMI at 530 eV and the narrow bandwidth has allowed to identify typical features of the water spectrum, such as the pre-peak observable at about 535 eV. In Fig. 4 we report a similar measurement done at the SSRL synchrotron [24] for comparison, and the results are in good agreement.

This proof-of-principle experiment paves the way for light-driven sub-ps dynamic studies in water and other molecules as well as in solid oxides by monitoring the time-resolved x-ray-absorption spectrum at the O K-edge.

REFERENCES

- [1] E. Allaria *et al.*, “Two-stage seeded soft-X-ray free-electron laser”, *Nat. Photonics*, vol. 7, pp. 913-918, 2013.
- [2] G. De Ninno *et al.*, “Single-shot spectro-temporal characterization of XUV pulses from a seeded free-electron laser”, *Nat. Comm.*, vol. 6, p. 8075, 2015.
- [3] K.C. Prince *et al.*, “Coherent control with a short-wavelength free-electron laser”, *Nat. Photonics*, vol. 10, pp. 176-179, 2016.
- [4] L.H. Yu, “Generation of intense uv radiation by subharmonically seeded single-pass free-electron lasers”, *Phys. Rev. A*, vol. 44, p. 5178, 1991.
- [5] E. Allaria and G. De Ninno, “Soft-X-Ray Coherent Radiation Using a Single-Cascade Free-Electron Laser”, *Phys Rev. Lett.*, vol. 99, p. 014801, 2007.
- [6] R.K. Lam *et al.*, “Soft X-Ray Second Harmonic Generation as an Interfacial Probe”, *Phys Rev. Lett.*, vol. 120, p. 023901, 2018.
- [7] H.-Y. Wang *et al.*, “Time-resolved observation of transient precursor state of CO on Ru(0001) using carbon K-edge spectroscopy”, *Phys. Chem. Chem. Phys.*, vol. 22, p. 2677, 2020.
- [8] E. Diesen *et al.*, “Ultrafast Adsorbate Excitation Probed with Subpicosecond-Resolution X-Ray Absorption Spectroscopy”, *Phys Rev. Lett.*, vol. 127, p. 016802, 2021.
- [9] G. Stupakov, “Using the Beam-Echo Effect for Generation of Short-Wavelength Radiation”, *Phys Rev. Lett.*, vol. 102, p. 074801, 2009.
- [10] P. R. Ribic *et al.*, “Coherent soft X-ray pulses from an echo-enabled harmonic generation free-electron laser”, *Nat. Photonics*, vol. 13, p. 555, 2019.
- [11] Z. Huang and K.-J. Kim, “Three-dimensional analysis of harmonic generation in high-gain free-electron lasers”, *Phys Rev. E*, vol. 62, p. 7295, 2000.
- [12] E.L. Saldin, E.A. Schneidmiller, and M. V. Yurkov, “Properties of the third harmonic of the radiation from self-amplified spontaneous emission free electron laser”, *Phys Rev. ST Accel. Beams*, vol. 9, p. 030702, 2006.
- [13] G. Penco *et al.*, “Nonlinear harmonics of a seeded free-electron laser as a coherent and ultrafast probe to investigate matter at the water window and beyond”, *Phys Rev A*, vol. 105, p. 053524, 2022.
- [14] I. Ben-Zvi, K.M. Yang, and L.H. Yu, “The fresh-bunch technique in FELs”, *Nucl. Instrum. Methods Phys Res. Sect. A*, vol. 318, p. 726, 1992.

- [15] D. Ratner *et al.*, “Second and third harmonic measurements at the linac coherent light source”, *Phys Rev. ST Accel. Beams*, vol. 14, p. 060701, 2011.
- [16] C. Svetina *et al.*, “PRESTO, the on-line photon energy spectrometer at FERMI: Design, features and commissioning results”, *J. Synchrotron Radiat.*, vol. 23, p. 35, 2016.
- [17] C. Ferrante *et al.*, “Non-linear self-driven spectral tuning of extreme ultraviolet femtosecond pulses in monoatomic materials”, *Light Sci. Appl.*, vol. 10, p. 92, 2021.
- [18] S. Reiche, “GENESIS 1.3: a fully 3D time-dependent FEL simulation code”, *Nucl. Instrum. Methods Phys. Res. Sect. A* vol. 429, 243, 1999.
- [19] S. Spampinati *et al.*, “Laser heater commissioning at an externally seeded free-electron laser”, *Phys Rev. ST Accel. Beams*, vol. 17, p. 120705, 2014.
- [20] O.Y. Gorobtsov *et al.*, “Seeded X-ray free-electron laser generating radiation with laser statistical properties”, *Nat Commun.* vol. 9, p. 4498, 2018.
- [21] O.Y. Gorobtsov *et al.*, “Statistical properties of a free-electron laser revealed by Hanbury Brown–Twiss interferometry”, *Phys Rev. A*, vol. 95, p. 023843, 2017.
- [22] R. Loudon, *The Quantum Theory of Light*, 3rd ed. (Oxford University Press, Oxford, 2000).
- [23] A.A. Lutman *et al.*, “Femtosecond x-ray free electron laser pulse duration measurement from spectral correlation function”, *Phys Rev. ST Accel. Beams*, vol. 15, p. 030705, 2012.
- [24] L-A. Näslund *et al.*, “X-ray absorption spectroscopy measurements of liquid water”, *J. Phys. Chem. B*, vol. 109, pp. 13835-13839, 2005. doi : 10.1021/jp052046q
- [25] F. Capotondi *et al.*, “Multipurpose end-station for coherent diffraction imaging and scattering at FERMI@Elettra free-electron laser facility”, *J. Synchrotron Radiat.*, vol. 22, p. 544, 2015.